

Identification and Isolation of Chlorhexidine Digluconate Impurities

Larry K. Revelle,^{1,3} William H. Doub,¹
Roger T. Wilson,² Monica H. Harris,¹ and
Aaron M. Rutter¹

Received July 9, 1992; accepted May 24, 1993

We report the identification of 11 impurities in variously stressed chlorhexidine digluconate (CHG) solutions. The structural assignment of each CHG impurity involved tentative identification from HPLC-MS data followed by synthesis of the appropriate standard, isolation of the impurity from the CHG solution by flash chromatography, and comparison of HPLC-MS, HPLC-UV, and NMR data of the impurity with the standard. Six of the synthetic impurity standards represent new compounds. Degradation studies of CHG solutions systematically stressed by heat, light, and low pH are reported with identification and approximate quantification of resulting impurities. Degradation mechanisms were proposed for each set of stress conditions applied to CHG solutions. Parallels were noted between the way CHG degrades in the thermospray interface of the HPLC-MS and the way CHG degrades with shelf time. Similarities were noted in the synthetic starting materials of CHG and the final degradation products.

KEY WORDS: chlorhexidine digluconate; impurities; identification; isolation; HPLC-MS; flash chromatography; HPLC-UV.

INTRODUCTION

Synthesis of chlorhexidine, 1,6-bis(*N*⁵-(*p*-chlorophenyl)-*N*¹-biguanido)hexane, was first reported by Rose and Swain in 1956 (1). Over the next four decades chlorhexidine has proven to be an effective antibacterial and disinfectant with many clinical applications (2,3). The digluconate, diacetate, and dihydrochloride salts of chlorhexidine are marketed under some 18 trade names (4). Several HPLC studies identify only one CHG impurity: *p*-chloroaniline (impurity C in this report) (5–7). Stevens *et al.* (8) identified two additional CHG impurities (one of which, *p*-chlorophenyl-diguanidine, is referred to as impurity D-2 in this report).

The purpose of our research was to identify and synthesize the major impurities in variously stressed CHG solutions. The synthesis and toxic properties (9) of impurity standards will be reported separately.

In this report the identification and isolation of 11 CHG impurities (Fig. 1) are discussed and CHG degradation mechanisms are postulated. Since many of the degradation products generated in stressed CHG solutions exists also in unstressed CHG solutions (Figs. 2A and B), any new analyte

identified in a CHG solution regardless of stress history is referred to in this paper as an impurity.

In manufacturing and clinical applications, CHG solutions are subjected to heat, light, and pH stresses of various magnitudes. In our studies CHG solutions are subjected to severe stresses: 100°C, direct sunlight, and 6 *M* HCl. We assert that the accelerated CHG degradation mechanisms described in this work parallel "real-life" CHG degradation mechanisms that take place at a slower rate under less severe stress conditions.

Our purposes was to identify and approximately quantify the CHG impurities. We compiled impurity profiles to match CHG stress conditions.

MATERIALS AND METHODS

Materials

The HPLC-grade methanol and hydrochloric acid were obtained from Fisher Scientific, St. Louis, MO. Glacial acetic acid and ammonium acetate were obtained from EM Science, Taylor Chemical Company, St. Louis, MO. Chlorhexidine digluconate (20%) solutions (stored at 5°C in the dark) were obtained from two proprietary sources and from Sigma Chemical Company, St. Louis, MO. The Lichroprep C18 packing material (25–40 mesh) was obtained from EM Science. The 50 mm × 45-cm flash-chromatography column was purchased from Ace Glass, Louisville, KY. The Zorbax CN HPLC column (150 × 4.6 mm, 7 μm) was obtained from Phenomenex, Torrance, CA. The water was purified through a Millipore system. The Pyrex culture tubes (16 × 150 mm) with screw-top lids and conical reaction vials with septa and "O" rings were purchased from Aldrich Chemical Company, as were deuterated NMR solvents, D₂O and CD₃OD.

Instrumentation

HPLC analyses were conducted on a Hewlett–Packard 1090M instrument equipped with a diode array detector and a Rheodyne manual injector (Model 7125). The HPLC-MS analyses were performed on a TSQ-70 mass spectrometer equipped with a thermospray ionization source from Finnigan MAT Corporation. A Waters 590 HPLC pump fitted with a Rheodyne manual injector (Model 7125) was employed. Nuclear magnetic resonance spectra were recorded on a Varian XL-300 (300 MHz) spectrometer.

HPLC Methods

HPLC-UV Method. Samples were injected manually onto the Zorbax CN column on the 1090M HPLC system at a flow rate of 1.5 mL/min (monitored at 230 nm because all the UV-active impurities absorb at this wavelength). The mobile phase ratio of buffer (0.1 *M* ammonium acetate, pH 5) to methanol ranged from 50:50 to 90:10 to facilitate resolution of the particular impurity of interest. In Fig. 2, each solution was analyzed twice: (a) a mobile phase ratio of 75:25 is employed to resolve most early-eluting peaks, and (b) a mobile phase ratio of 65:35 resolves the later-eluting impurity peaks.

¹ Food and Drug Administration, Division of Drug Analysis, 1114 Market Street, Room 1002, St. Louis, Missouri 63101.

² U.S. Department of Agriculture, FSIS Midwestern Laboratory, P.O. Box 5080, St. Louis, Missouri 63115.

³ To whom correspondence should be addressed.

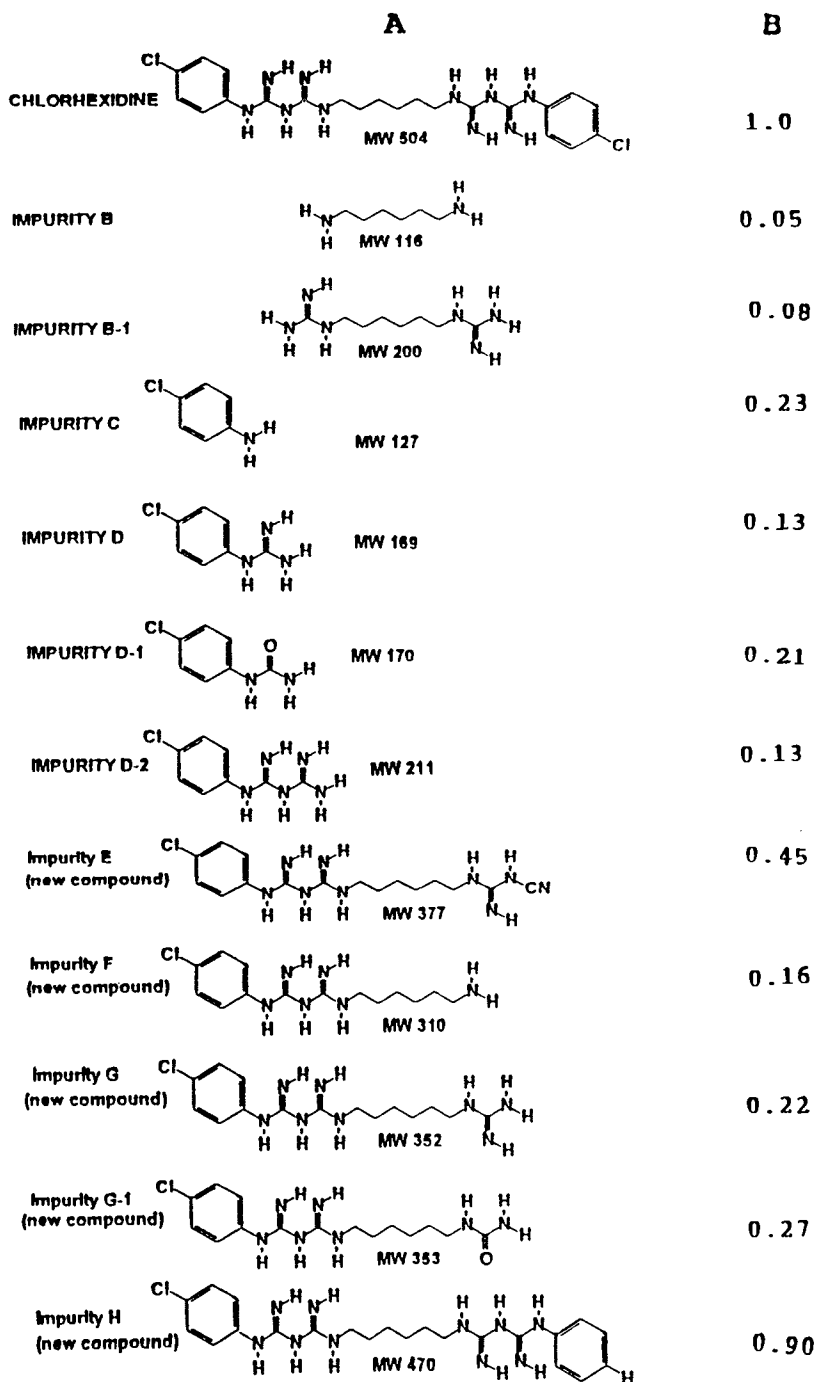


Fig. 1. (A) CHG impurity structures. (B) Retention times relative to chlorhexidine (1.0) under standard HPLC-UV conditions with a mobile phase ratio of 65/35. Retention times for non-UV-active impurities B and B-1 were extrapolated from HPLC-MS data.

HPLC-MS Method. Samples were injected manually onto the Zorbax CN column with a Waters 590 HPLC pump at a flow rate of 1.0 mL/min with the same mobile phase as employed in the HPLC-UV method. The column was connected directly to the Finnigan TSQ-70 mass spectrometer. The thermospray vaporizer temperature was 80°C, the jet temperature was 220°C, the block-temperature reading was 175°C, and the aerosol temperature was 210°C.

We were unable to devise one single gradient method which would resolve all impurities. Isocratic methods saved time in analyzing large numbers of complex CHG solutions. The key was to fit the isocratic mobile phase ratio to the impurity investigated.

NMR Method

Impurity standards, isolated impurities, and degraded

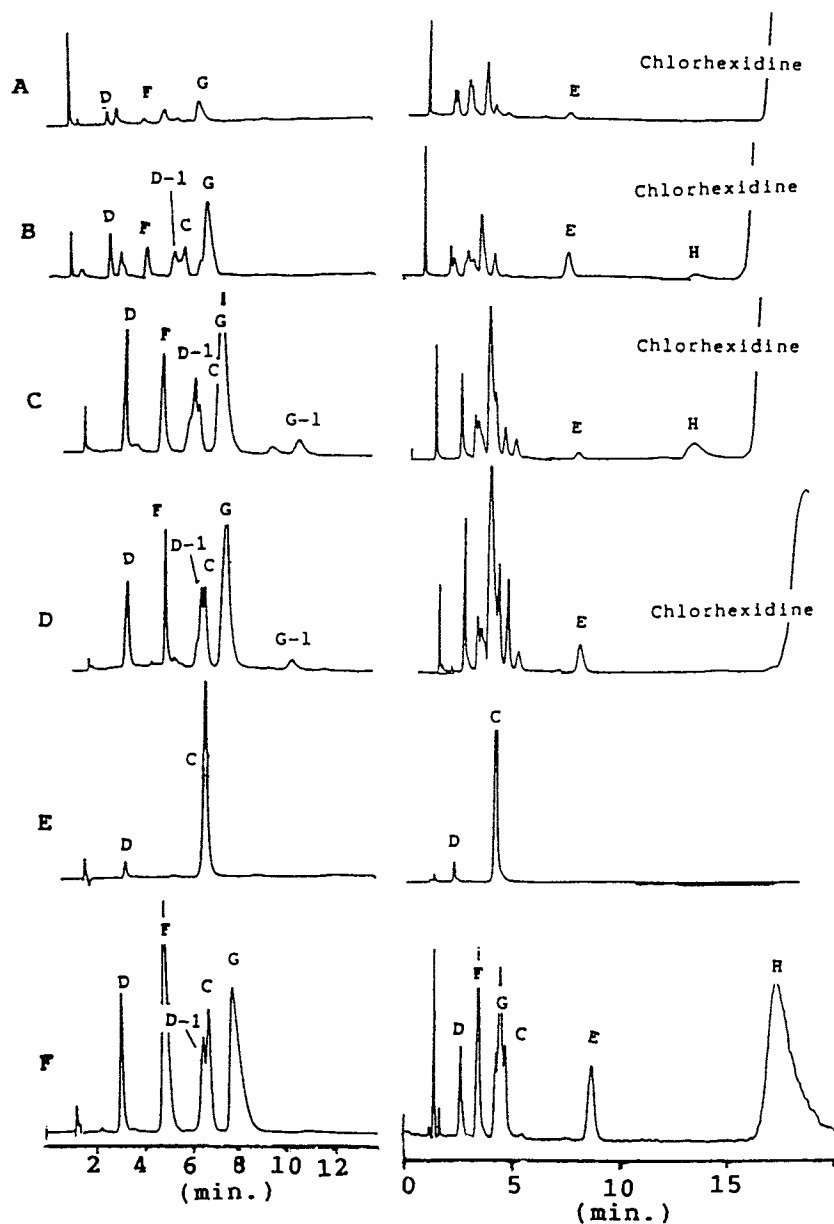


Fig. 2. Chromatograms of CHG solutions under standard HPLC-UV conditions. Each solution was injected, first, with a mobile phase ratio of 75/25 to resolve early-eluting impurities and, second, with a mobile phase ratio of 65/35 to resolve later-eluting impurities. (A) Unstressed synthetic CHG (20%). (B) Unstressed commercial CHG (20%). (C) Commercial CHG (20%) subjected to room light for 2 years. (D) Commercial CHG (20%) subjected to 100°C for 1 day. (E) Commercial CHG (20%) subjected to 100°C/6 *M* HCl for 1 day. (F) CHG impurity standards.

CHG solutions, in D_2O or CD_3OD solvents, were analyzed at a proton resonance frequency of 299.94 MHz at 24°C. Collection conditions included 16 transients, a 30° flip angle pulse, and an acquisition time of 2 sec.

Isolation of CHG Impurities by the Flash-Chromatography Method

As an example, the isolation of impurity G is given. A commercial 20% CHG solution (400 g), which had been

heated to 95°C for 7 hr, was divided into four portions and passed in parallel through two flash chromatography columns (50 mm × 45 cm), each packed with 100 g of LiChroprep C-18 packing material. The mobile phase was water: methanol (90:10), the head pressure (nitrogen) was 10 psi, and the flow rate was 10–20 mL/min. Each fraction was analyzed by the HPLC-UV method previously described. The best fractions were combined and rechromatographed a total of three times until approximately 2.5 g (3.8% yield) of the digluconate salt of impurity G was isolated at a purity

level of 97% by integrated area. The ^1H NMR spectrum of this isolated sample of impurity G was obtained to compare with the NMR spectrum of synthetic standard G.

General Method for Identifying CHG Impurities

The general procedure for identification of a given CHG impurity includes five steps. (a) From a careful literature study of CHG synthetic methods and known degradation mechanisms of compounds having structures similar to that of CHG, a list of likely CHG impurities was compiled for reference. (b) Based on HPLC-MS data and the above reference list, a tentative structural identification was made (Fig. 3). (c) A standard was synthesized to fit the structural requirements postulated in step b. (d) The identity of the impurity was confirmed by matching the chromatographic and spectroscopic properties of the impurity with those of the standard (Figs. 2–5). (e) The impurity was isolated from the CHG solution by flash chromatography as described above in the previous section. Characterization of the isolated impurity by NMR and a comparison to the NMR spectra of the standard provided additional proof of structure of the CHG impurity (Fig. 5 and NMR Characterization of Isolated Impurity G, below).

Several impurities (especially G, G-1, and H) showed a sensitivity to column overload (as peak height increases, retention time decreases). In addition, the true retention times of certain impurities (especially H) were altered by proximity to the overload CHG peak. The elution order of the impurities was shown to vary with the age and lot number of the column and the mobile phase ratio (impurities C and G com-

mute in elution order as the mobile phase ratio changes from 75:25 to 65:35). Therefore, the identity of an impurity was confirmed by spiking the standard impurity into CHG impurity solution rather than matching retention time numbers from different solution injections.

In addition, the use of diode array detection to identify impurity peaks by matching UV spectra was critical. In the same way, identification of impurity peaks by HPLC-MS (Fig. 3 and 4) was invaluable. No sample preparation was required by either method.

Degradation Studies

Thermal-Stress Method. Approximately 1 g of unstressed commercial CHG (20% solution) (Fig. 2B) was placed in each of two Pyrex culture tubes with Teflon-lined screw caps. The tubes were placed in an oven at 100°C . A single tube was removed at each 24-hr interval over a 2-day period. The thermally stressed CHG solution was immediately analyzed by the HPLC-UV method (Fig. 2D) and the HPLC-MS method (Fig. 3).

Strong Acid-Stress Method. Approximately 1 g of commercial CHG (20% solution) (Fig. 2B) and 1 g of 6 M HCl were placed into each of two 5-mL conical vials with septums and "O" rings. The vials were placed in an oven at 100°C . A vial was removed at day 1 and day 2. Each vial was analyzed in the same way. A syringe needle was inserted through the septum to withdraw the headspace gases. The gases were bubbled through a saturated solution of calcium hydroxide.

Each reaction solution was divided into two portions.

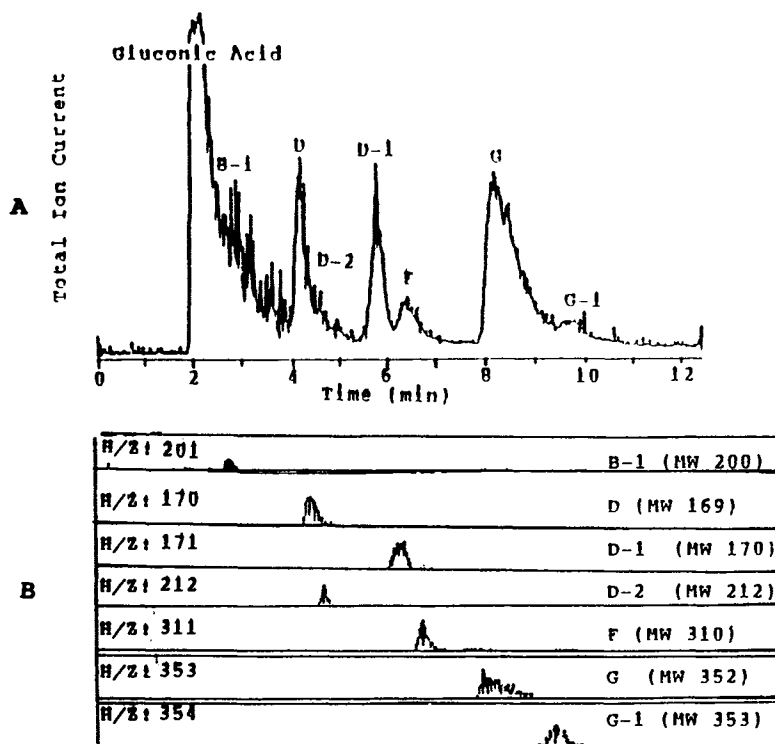


Fig. 3. (A) HPLC-MS chromatogram of a CHG solution subjected to 95°C for 7 hr injected under standard conditions with a mobile phase ratio of 80/20. (B) Single-ion monitoring of the $M + H$ ion for each impurity detected.

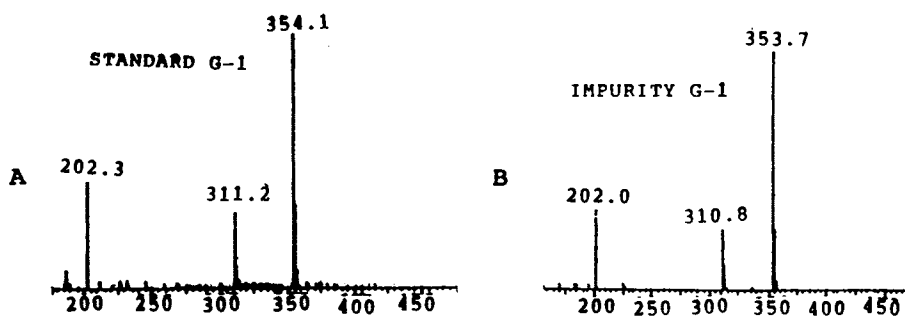


Fig. 4. HPLC-MS spectrum standard conditions with a mobile phase ratio of 80:20. (A) Synthetic standard G-1. (B) Impurity G-1.

(a) One portion was analyzed by HPLC-UV (Fig. 2E) and by HPLC-MS. (b) The remaining portion was evaporated to a brown solid under pressure and placed in a vacuum desiccator overnight to remove residual water and HCl. The residue was dissolved in D_2O and 1H NMR was obtained (Fig. 5C). MNR spectra of impurity C and impurity B-1 standards were obtained for comparison (Figs. 5A and B).

Light-Stress Method. Approximately 1 g of unstressed CHG (20% solution), freshly prepared by a proprietary method from analytical-grade reagents with minimum stress (Fig. 2A), was placed into each of 10 Pyrex culture tubes with Teflon-lined screw caps. The tubes were positioned to receive the direct rays of the summer sun for 69 sunlight hr (temperature $32^\circ C$). At certain time intervals, a single tube was removed and analyzed by the HPLC-UV method and the HPLC-MS method.

RESULTS

Typical HPLC-UV Chromatogram

An unstressed commercial CHG solution (20%) (Fig. 2B), blackened by storage on the benchtop for 2 years at room temperature with no protection from ordinary room light (fluorescent lamps), was injected under standard HPLC-UV conditions, once with a mobile phase ratio of

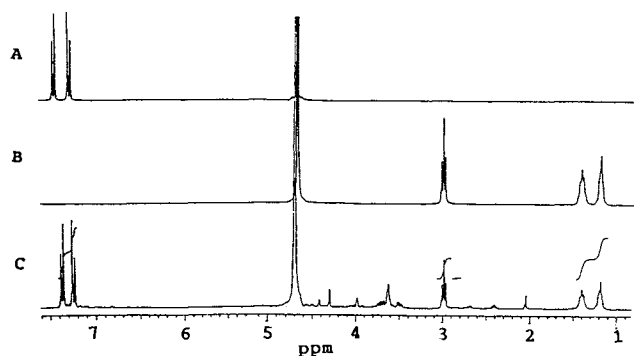


Fig. 5. 1H NMR spectra, from samples dissolved in D_2O , were referenced to the HOD resonance at 4.7 ppm. (A) Impurity C standard (*p*-chloroaniline hydrochloride). (B) Impurity B-1 standard (1,6-bisguanidinohexane dihydrochloride). (C) CHG solution digested with 6 M HCl at $100^\circ C$ for 1 day. A weak triplet resonating at 2.85 ppm verifies the presence and relative concentration of impurity B. The resonances of impurity B-1 indicate its relative concentration and verify its presence by lining up with the standard B-1 resonances.

75:25 and again with a mobile phase ratio of 65:35 (Fig. 2C). The chromatogram resulting from the first injection shows impurities D, F, G, and G-1 fairly well resolved. Impurities C and D-1, while only partially resolved under the conditions employed, can be resolved completely using a mobile phase ratio of 90:10. The chromatogram resulting from the second injection (mobile phase ratio of 65:35) shows the later-eluting impurities E and H and chlorhexidine itself. Note that under conditions of significant light stress, the impurity H concentration increases sharply.

Typical HPLC-MS Chromatogram

An unstressed commercial CHG solution (20%) (Fig. 2B) heated to $95^\circ C$ for 10 hr was injected into the HPLC-MS system under the conditions previously defined with a mobile phase ratio of 80:20 to afford the chromatogram in Fig. 3A. Impurity B-1, invisible to HPLC-UV detection, is seen. The fact that impurities C and D-1 are not well resolved under HPLC-UV (Figs. 2C and D) is no problem in this chromatogram because impurity C is insensitive to thermospray detection, while D-1 shows a good sensitivity. The very intense peak at the solvent front is due to gluconic acid, the counter ion to chlorhexidine in CHG. Gluconic acid is UV transparent at 230 nm.

In Fig. 3B, the single ion monitoring of the M + H ion of impurities B-1, D, D-1, D-2, F, G, and G-1 are seen. In addition the relative retention times are confirmed. For example, the M + H of D-2 is apparent even though D and D-2 coelute.

Methods by Which CHG Impurities Were Identified

Of the 11 impurities identified in CHG solutions (Fig. 1), 6 (D, D-1, E, F, G, and H) were identified by the rigorous five-step method previously outlined under General Method for Identifying CHG Impurities (above). The five-step method was applied to those major impurities that were UV active, detectable by thermospray MS, and stable enough to synthesize and isolate. Impurity B, which is not UV active, was identified by HPLC-MS and NMR (Fig. 5C). Impurity C, which is insensitive to thermospray MS, was identified by HPLC-UV and NMR (Figs. 2 and 5). Impurity B-1, which is not UV active, was identified by a comparison of the synthetic standard with the impurity by HPLC-MS (Fig. 3) by NMR (Fig. 5). Impurities G-1 and D-2, which are not major impurities, were not isolated from the stressed CHG solution; however, they were identified by a comparison of the

synthetic standards with the impurities by HPLC-UV and HPLC-MS (Figs. 3 and 4).

Each impurity showed a $M + H$ ion to match the corresponding standard with the exception of impurity C. We postulate that *p*-chloroaniline is insensitive to thermospray MS because, in contrast to the other impurities, only one site for protonation is available and this site is not resonance stabilized.

NMR Characterization of Isolated Impurity G

The ^1H NMR of isolated impurity G digluconate was obtained in CD_3OD . Ignoring the resonances of the gluconic acid counterion (multiplets $\delta 3.6\text{--}4.2$), the isolated impurity G resonances are $\delta 1.40$ (4H, m, $-\text{CH}_2-\text{CH}_2-\text{CH}_2-\text{CH}_2-$), $\delta 1.60$ (4H, m, $-\text{CH}_2-\text{CH}_2-\text{CH}_2-\text{CH}_2-$), $\delta 3.20$ (4H, m, $-\text{CH}_2-\text{CH}_2-\text{CH}_2-\text{CH}_2-$), $\delta 7.3$ (2H, d, $J = 8$ Hz, Ar-H), $\delta 7.42$ (2H, d, $J = 8$ Hz, Ar-H). Ignoring the resonances of the acetic acid counterion (singlet $\delta 1.95$) of the synthetic G diacetate standard in CD_3OD , the resonances of standard G were identical to those of impurity G with respect to splitting patterns and integrals. Only small changes in chemical shift of less than 0.1 ppm were noted at $\delta 1.6$ and $\delta 3.2$ due to differences in the acidity of the respective counterions.

Overview of the CHG Degradation Studies

The purpose of the CHG degradation studies was to identify and approximately quantitate the impurity profiles matched up with CHG stress conditions. The percentages of impurities reported are expressed as integrated area percents based on HPLC-UV chromatograms. No corrections were made for individual differences in UV molar absorptivity from one impurity to the next (all UV active impurities contain variations of the same *p*-chlorophenyl chromophore). In addition, NMR was employed to find the molar ratios of impurities C, B-1, and B (Fig. 5C).

Unstressed CHG Solutions. The commercial CHG solutions (Fig. 2B) and the freshly prepared synthetic CHG solutions (Fig. 2A) were stored at 5°C in the dark. The unstressed commercial CHG solutions showed higher impurity levels than the freshly prepared solutions. In the commercial solutions the impurities identified were D, D-1, F, C, G, E, and H, which account for about 1–2% of the total UV activity. The dominant impurity was G (ca. 0.6%). In the synthetic CHG solutions the impurities identified were D, F, G, and E, which account for about 0.5% of the total UV activity. Again, the dominant impurity was G (ca. 0.2%).

Synthetic CHG solutions were employed in the sunlight degradation studies because these solutions showed no impurity H (in contrast to the commercial CHG solutions). It was important to show that impurity H results from light stress and not from thermal stress. In the thermal- and acid-stress experiments the commercial CHG solutions proved adequate.

Thermally Stressed CHG Solutions. Figure 6A shows the thermal decomposition of CHG over a 2-day period at 100°C . Figure 2D is a HPLC-UV chromatogram of the CHG solution stressed for 1 day at 100°C . The concentrations of impurities C, D, D-1, and G increase more rapidly than those

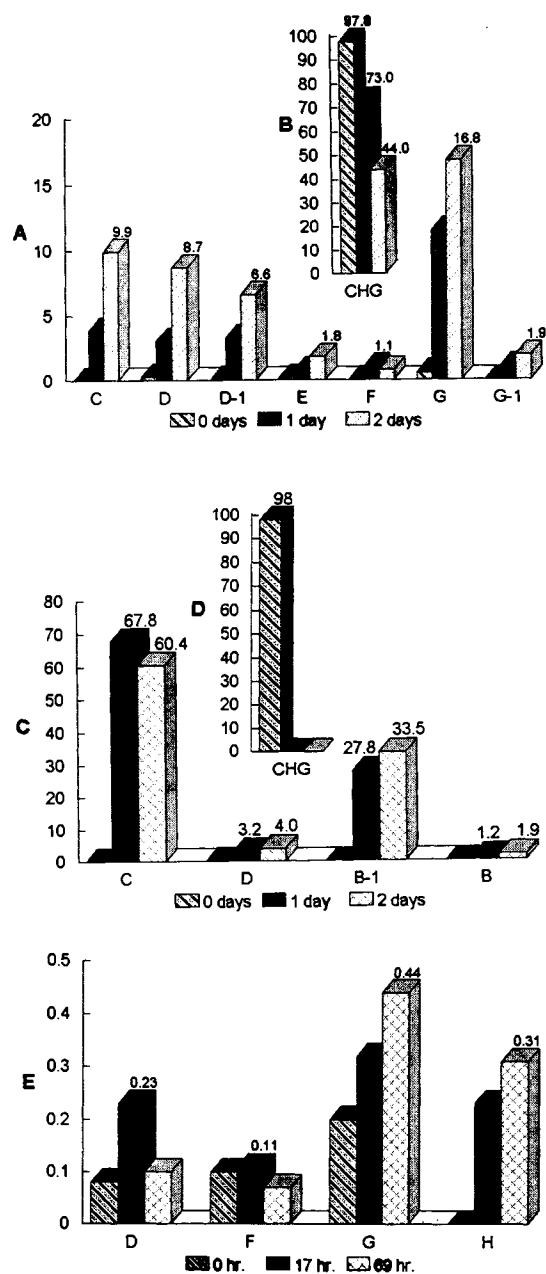


Fig. 6. Graphs of CHG impurities quantified (as mole percentage units) by integration of HPLC-UV peaks compared to total UV integration. In graph C, integration of NMR resonances was used to supplement HPLC integrations in determining molar ratios. (A) Impurity profile of a CHG solution heated to 100°C . (B) Degradation of CHG at 100°C . (C) Impurity profile resulting from a CHG solution stressed with 100°C and 6 M HCl . (D) Degradation of CHG at 100°C with 6 M HCl . (E) Impurity profile resulting from direct sunlight exposure of CHG solution.

of the other impurities. It is postulated that D and G accumulate as a result of a retere reaction (13) (Fig. 7A), D-1 and G-1 result from hydrolyses of D and G, respectively (14,15), and C results from hydrolysis and decarboxylation reactions (15,17,18) (Fig. 7B). The amount of intact CHG is reduced by more than 50% in 2 days under these conditions (Fig. 6B).

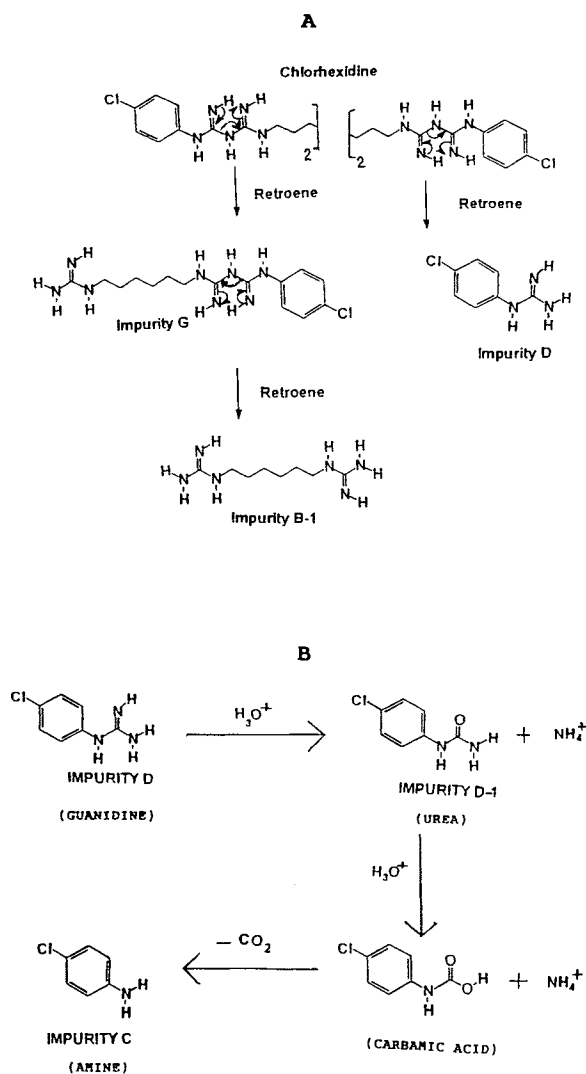


Fig. 7. CHG degradation mechanisms. (A) Thermal degradation via retroene reaction. (B) Hydrolysis of guanidine intermediates to final amines.

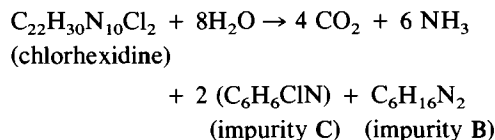
CHG Solutions Stressed by Strong Acid. Two vials of a CHG solution (20%) were digested with 6 M HCl at 100°C for 1 and 2 days, respectively. Each vial was analyzed in the same way. The headspace gases that accumulate were injected into saturated lime water to give an immediate precipitate, indicating the presence of carbon dioxide.

The day 1 reaction solution was analyzed by HPLC-UV analysis (Fig. 2E) to reveal only two UV active materials, impurity C (96%) and impurity D (4%); under the same analytical conditions the day 2 reaction solution showed no significant change. Each reaction solution was analyzed by HPLC-MS to show significant amounts of impurities B and B-1 (each impurity matched the corresponding standard with respect to $M + H$ ion and retention time).

The day 1 and day 2 reaction solutions were analyzed by NMR. The major resonance patterns of impurities C and B-1 matched the resonances of the corresponding standards (Fig. 5). (The resonances from $\delta 3.4$ to $\delta 4.0$ are due to gluconic acid residues). The resonances of impurity B were established by spiking standard B into the degraded CHG solu-

tions. By correlating the NMR integrations with the HPLC integrations, the relative molar ratio of each impurity (D, C, B-1, and B) at day 1 and day 2 was calculated and recorded in Fig. 6C. It was noted by NMR and by HPLC that all traces of CHG had degraded by day 1 (Fig. 6D).

It is postulated that heat breaks down the CHG by the retroene reaction (13) into guanidines D and B-1 (Fig. 7A). Subsequently, these guanidines are hydrolyzed through urea and carbamic acid intermediates to amines C and B, respectively (Fig. 7B). From Fig. 6C it is apparent that the hydrolysis of guanidine D to amine C (essentially complete after 1 day) is much faster than the hydrolysis of guanidine B-1 to amine B. The observation that the concentration of B at day 2 is nearly twice that of day 1 shows that the hydrolysis of B-1 to B is still in progress. The decarboxylation of the carbamic acid intermediates is verified by the collection of carbon dioxide in each vial. The concentration of impurity C in each vial solution is essentially the same at day 2 as at day 1, indicating the stability of amine C. We postulate that the final degradation products by hydrolysis are amines C and B (17,18). The following balanced equation for the thermal/acid catalyzed CHG degradation is given:



Ironically, *p*-chloroaniline (impurity C) and 1,6-hexanediamine (impurity B), the end-product degradation impurities, are also the principal starting materials in the synthesis of chlorhexidine (1).

Sunlight-Stressed CHG Solutions. Figure 6E shows the sunlight-catalyzed degradation of CHG over a 69-hr period. The impurity profile generated is not significantly different from the impurity profile generated under thermal conditions except for the sharp increase in impurity H. Impurity H was not seen in the thermal degradation studies. It is postulated that impurity H is a photodegradation product. It was noted that CHG solutions tend to turn yellow and darken after 34 hr of direct sunlight exposure. Since the temperature of the CHG solutions was 32°C during the exposure, some of the degradation could be viewed as thermal.

CHG Solutions Stressed by Thermospray MS Vaporizer Probe. The injection of an analytically pure CHG solution into the HPLC-MS system resulted in a mass spectrum showing the protonated parent chlorhexidine molecule (m/e 505, 30%) and several very prominent ion clusters corresponding to the protonated parents of the major CHG impurities: B-1 (m/e 201, 100%), D (m/e 170, 18%), and G (m/e 353, 70%). The additional ion clusters indicate the chlorhexidine molecules have undergone unimolecular thermal-degradation processes in the vaporizer probe of the thermospray interface (175°C). As the eluant flashes through the heated metal capillary interface, the solvent is rapidly volatilized, leaving the protonated parent ions to enter the ion chamber of the mass spectrometer (12). A large percentage of the chlorhexidine molecules that enter the vaporizer probe undergoes unimolecular retroene reactions to generate some of the same decomposition products that also accumulate as CHG solution degrade thermally in real life (Fig. 7A).

DISCUSSION

We propose that impurity G is the dominant decomposition product under thermal stress because it is formed by a retroene reaction through a resonance-stabilized, six-electron transition state (13) (Fig. 7A). One of the most important structural features of the chlorhexidine molecules is the large number of conveniently available retroene decomposition routes: chlorhexidine decomposes by the retroene reactions to give guanidine G, guanidine D, and bisguanidine B-1. Since impurity G is the dominant impurity in solutions stored at room temperature, it may be that the retroene reaction takes place even at 25°C.

In Fig. 7B, the hydrolytic decomposition of chlorhexidine intermediates is shown. Guanidines hydrolyze to ureas, ureas hydrolyze to carbamic acids, and transient carbamic acids decarboxylate to amines (17,18). Hydrolysis reactions take place under neutral conditions (Fig. 6A) as shown by the presence of ureas D-1 and G-1 and amines F and C; however, in Fig. 6C, the high concentration of final hydrolysis product, amine C, the significant increase in concentration of amine B at day 2, and the buildup of carbon dioxide in both vials indicate that the hydrolysis mechanisms dominate under acid conditions. The hydrolysis of aromatic guanidine D is much faster than the hydrolysis of aliphatic guanidine B-1.

In Figs. 2C and 6E, it is obvious that light-catalyzed CHG degradation results in high concentrations of impurity H. Since impurity H does not form under thermal- or acid-stress conditions, apparently light causes cleavage of the carbon-chloride bond at the aromatic ring, resulting in a free radical intermediate. Sethi *et al.* also propose a free radical mechanism for the exchange of aromatic halides with hydrogen (16). The observation that CHG solutions darken upon exposure to light but remain colorless under thermal stress is another indication that a free radical mechanism may be in operation. Moore points out that photohalogenation of aromatic compounds is a well-documented reaction (19).

Of the 11 impurities reported, at least 7 of them exist in unstressed commercial CHG solutions (Fig. 2B). For the most part, the severe stress conditions served to increase the concentration of impurities already present and to clarify the degradation mechanisms.

ACKNOWLEDGMENTS

We would like to acknowledge the assistance of Richard Zerfing, John Reepmyer, and Walter Zielinski in reading the manuscript, checking the calculations, and offering suggestions.

REFERENCES

1. F. L. Rose and G. Swain. Bisdiguanydes having antibacterial activity. *J. Chem. Soc.* 4422-4425 (1956).
2. S. E. Davies, J. Francis, A. R. Martin, F. L. Rose, and G. Swain. 1,6-Di-4-chlorophenyldiguanydohexane ("Hibitane"). Laboratory investigation of a new antibacterial agent of high potency. *Br. J. Pharmacol.* 9:192-196 (1954).
3. Chlorhexidine in the prevention and treatment of gingivitis. H. Loe (ed). *J. Periodont. Res.* 21(Suppl. 16):1-89 (1986).
4. Chlorhexidine. In S. Budavari, M. J. O'Neill, A. Smithy, and P. E. Heckelman (eds.), *The Merck Index*, 11th ed., Merck and Co., Rahway, NJ, 1989, p. 323.
5. M. Hoang, J. F. Moellmer, and M. A. Khan. Separation of chlorhexidine breakdown products including 4-chloraniline in surgical scrubs containing chlorhexidine. *J. Liq. Chromatogr.* 13:2677-2687 (1990).
6. *British Pharmacopoeia*. Her Majesty's Stationery Office, London, England, 1973, p. 98.
7. M. Bauer, C. DeGude, and L. Mailhe. Simultaneous determination of chlorhexidine, tetracaine and their degradation products by ion-pair liquid chromatography. *J. Chromatogr.* 315:457-464 (1984).
8. L. Stevens, J. R. Durwachter, and D. O. Helton. Analysis of Chlorhexidine sorption in soft contact lenses by catalytic oxidation of (¹⁴C)chlorhexidine and by liquid chromatography. *J. Pharm. Sci.* 75:83-86 (1986).
9. C. Long, T. Martinez, L. Revelle, T. Layloff, and P. Reed. Comparison of the toxicity of contaminants found in commercial chlorhexidine formulations. Paper presented to Western Pharmacological Society Congress, Jan. 11 (1992).
10. W. C. Still, M. Kahn, and A. Mitra. Rapid chromatographic technique for preparative separations with moderate resolution. *J. Org. Chem.* 43:2923-2925 (1978).
11. R. M. Ladd and A. Taylor. Combining overload flash chromatography and high-resolution preparative liquid chromatography to isolate low-level synthetic bulk drug impurities. *LC-GC* 7:584-586 (1989).
12. K. J. Volk, R. A. Yost, and A. Brajter-Toth. Electrochemistry on line with mass spectroscopy. *Anal. Chem.* 64:21A-33A (1992).
13. H. M. R. Hoffman. The ene reaction. *Angew. Chem. Int. Ed. Engl.* 8:556-577 (1969).
14. V. G. Granik and S. I. Kaimanakoua. Advances in chemistry of amidines. *Russ. Chem. Rev.* 52:669-703 (1983).
15. J. M. Sayer and P. Conlon. The timing of the proton-transfer process in carbonyl additions and related reactions. General-acid-catalyzed hydrolysis of imines and n-acylimines of benzophenone. *J. Am. Chem. Soc.* 102:3592-3602 (1980).
16. S. K. Sethi, C. C. Nelson, and J. A. McCloskey. Dehalogenation reactions in fast atom bombardment mass spectroscopy. *Anal. Chem.* 56:1975-1977 (1984).
17. D. P. N. Satchell and R. S. Satchell. Acylation of ketens and isocyanates. A mechanistic comparison. *Chem. Soc. Rev.* 4:231-250 (1975).
18. W. Huber. Determination of carboxylic acid derivatives via acidic hydrolysis. *Mikrochim. Acta* 5:897-904 (1969).
19. D. E. Moore. Principles and practice of drug photodegradation studies. *J. Pharm. Biomed. Anal.* 5:441-453 (1987).